

Modification of the gold/graphite interfacial energy by interfacial adsorption of nickel

U. GANGOPADHYAY and P. WYNBLATT

Department of Materials Science and Engineering, Carnegie Mellon University, Pittsburgh, PA 15213, USA

The effects of nickel additions on the energy of gold/graphite interfaces was investigated. Nickel was found to segregate to the interface forming an adsorbed layer. Solid-state wetting measurements showed that the contact angle of gold on graphite was decreased by 7.8° by the addition of 15 at% Ni. The corresponding decrease in interfacial energy, determined from the Young–Dupré equation was found to be $\sim 112 \text{ mJ m}^{-2}$. The interfacial excess of nickel corresponding to 15 at% Ni in the bulk was calculated by means of the Gibbs adsorption isotherm to be about 0.45 equivalent monolayers of gold. The presence of nickel at the interface was further confirmed by crater-edge profiling studies performed in a scanning Auger microprobe.

1. Introduction

The interfaces between metals and non-metallic solids play an important role in determining the properties of many systems, such as microelectronic components, metal–matrix composites, and metal–ceramic joints. In the context of mechanical behaviour, the so-called work of adhesion is often considered to provide a metric of interfacial strength. The work of adhesion represents the energy change which results if an interface is separated to produce two surfaces. Thus, other things being equal, a lowering of interfacial energy generally leads to mechanically stronger interfaces. Control of interfacial energy in such systems is therefore of considerable practical interest. One way that interfacial energy can be controlled in metal–non-metal systems is through judicious alloying of the metallic constituent with interface active elements, which segregate to the interface thereby decreasing the interfacial energy.

There have been many studies of the effects of alloying on interfacial energy in metal–ceramic and metal–carbon systems. Most of these studies have evaluated the effects of alloying on interfacial energy by means of wetting measurements of liquid metals and alloys on a variety of substrates [1–5]. Major improvements in wetting due to alloying were generally attributed to the formation of reaction products at the interface. The previous wetting studies suffer from several shortcomings. First, previous experimental studies were generally performed under conditions where contamination of the surfaces and interfaces could neither be ensured nor even monitored. Because impurity adsorption can influence both surface and interface energetics, the reliability of those studies is uncertain. Second, the energetics of liquid–solid interfaces are expected to differ from those of solid–solid interfaces. Third, the lowering of interfacial energy by alloying with elements which result in interfacial reac-

tions can lead to the formation of brittle interfacial reaction products which may lead, in turn, to mechanically weaker, rather than stronger, interfaces. Recently, we have attempted to address the uncertainties of previous studies by undertaking solid-state wetting studies under conditions of ultrahigh vacuum (UHV), so as to control surface and interface cleanliness [6]. Furthermore, the studies have been performed under conditions where surface and interface composition could be monitored by surface analytical techniques. Finally, alloying additions to the metal component were chosen so as to promote interfacial segregation, without the formation of bulk interfacial reaction products.

Our initial study was performed on the lead–graphite system [6] in which interfacial energy changes were effected by alloying the lead with nickel. However, the maximum solubility of nickel in lead amounts to a mere 0.6 at% [7]. In the present study we report the results of an investigation of the effects of nickel additions to the gold–graphite system on the gold/graphite interfacial energy. This system was selected because nickel and gold are soluble in all proportions at high temperatures [8]; and even at lower temperatures, the solubility of nickel in gold is considerably larger than that of nickel in lead.

Nickel was selected as an alloying addition based on its higher affinity for carbon than gold. This provides a driving force for segregation of nickel to the gold/graphite interface. In addition, neither nickel nor gold form thermodynamically stable carbides, thus avoiding the formation of possibly brittle interfacial reaction products.

2. Conceptual considerations

The solid-state wetting approach used in this study is based on the sessile drop technique, but differs from it

in several important regards. In the sessile drop technique, a relatively large liquid drop (a few millimetres in diameter) is equilibrated on a substrate. The shape of the drop is the result of a balance between surface tension forces, which tend to make the drop spherical, and gravity forces which tend to flatten the drop. The surface tension of the drop can be obtained from the mass of the drop and the degree of flattening. If the surface energy of the substrate is known, a simultaneous measurement of the contact angle can yield the energy of the drop/substrate interface through the application of the Young–Dupré equation

$$\gamma_{\text{int}} = \gamma_s - \gamma_m \cos \theta \quad (1)$$

which relates the metal/substrate interfacial energy, γ_{int} , to the surface energies of the metal, γ_m , the substrate, γ_s , and the contact angle, θ , as illustrated in Fig. 1. The sessile drop technique cannot be used for solids, because their high effective viscosity leads to infinitesimally slow rates of equilibration of the drop shape. One way of increasing kinetics of shape equilibration is to decrease the size of the drop from millimetres to micrometres (because the rate of shape equilibration by surface diffusion, for example, depends on particle radius raised to the fourth power [9]). However, for such small particles, surface tension forces dominate, and any flattening due to gravity is far too small to measure. Nevertheless, if the surface energies of both the solid droplet and the substrate are known, then a measurement of contact angle can be used, together with the Young–Dupré equation, to calculate the interfacial energy between the solid droplet and the substrate. Another important difference between this approach and conventional sessile drop measurements is that the experiments were conducted in UHV under conditions where surface compositions could be monitored by Auger electron spectroscopy. These composition measurements are important, as any adsorption or segregation at these surfaces must be quantified so as to correct the surface energies of the pure components by means of the Gibbs adsorption isotherm, before the Young–Dupré equation is used to calculate the interfacial energy. The Gibbs

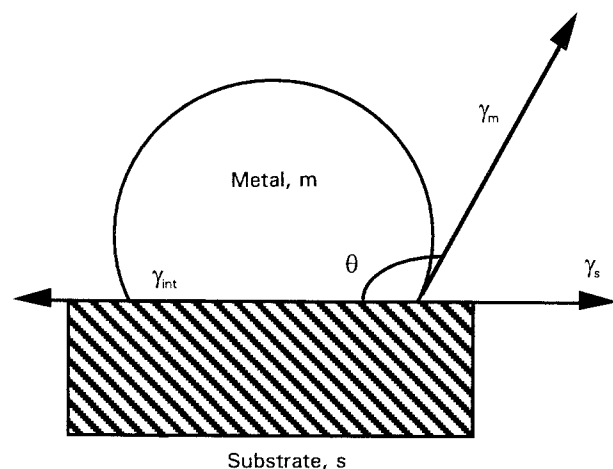


Figure 1 Crystallite of metal, *m*, in equilibrium with a substrate, *s*.

adsorption isotherm may be expressed as [10]

$$d\gamma = \sum_{i=1}^n \Gamma_i d\mu_i \quad (2)$$

where Γ_i and μ_i are the surface excess concentration and the chemical potential of the *i*th component, respectively. The composition of the interface may then be obtained by a second application of the Gibbs adsorption equation to the change in interfacial energy with bulk composition [10].

3. Experimental procedure

3.1. Sample preparation

The samples prepared consisted either of pure gold on graphite or of Au–15 at % Ni on graphite. The preparation procedure was substantially similar to that of our earlier study on lead/graphite [6]. Graphite flakes with (0001) surfaces were prepared by cleaving off a highly textured pyrolytic graphite block. These flakes were inserted into folding TEM grids and mounted on to a tantalum strip which could be heated by passage of current. This assembly was introduced into a UHV system containing two evaporation sources for deposition of gold (99.999%) and nickel (99.999%). The UHV system had a base pressure of 10^{-10} torr (1 torr = 133.322 Pa). After evacuation, the graphite substrates were heated for cleaning and degassing to a temperature of 1200 °C for 4 h. The graphite substrates were then cooled to room temperature, following which gold or gold and nickel were deposited on to the substrates by physical vapour deposition. The deposition of the alloy was such that nickel was sandwiched between layers of gold. This ensured that no nickel was initially present at the gold/graphite interface or at the free gold surface. The rates of deposition and the total amount deposited were monitored with a precalibrated, vibrating crystal film-thickness monitor to produce 1 μm thick films. Some of these thin-film samples were equilibrated at 850 °C for 5 h, long enough to achieve near-equilibrium solute distribution in the bulk of the films as well as at the film/graphite interface [11]. The time and temperature of this heat treatment were high enough to reach compositional equilibrium in reasonable times, while at the same time low enough to avoid significant losses of gold by evaporation. These samples will be referred to as thin-film samples.

Other samples of either pure gold or of the alloy were flash-heated to a temperature just above the melting point to dewet the film into discrete islands, and then cooled rapidly to avoid evaporation losses. This process produced islands 1–5 μm in size which solidified epitaxially on the substrate such that the {111} planes of the islands were parallel to the {0001} planes of the graphite. These samples will be referred to as island samples. Both types of sample were then taken out of the UHV system for further manipulations, as described below.

3.2. Wetting experiments

The island samples were wrapped in gold foil, then reinserted into the UHV chamber and heated to

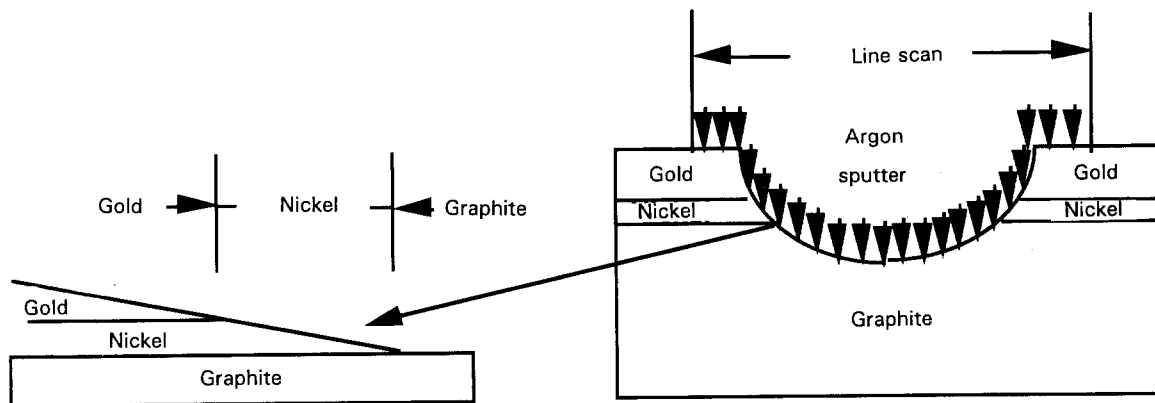


Figure 2 Schematic representation of the crater-edge profiling technique.

850 °C for 27 h in order to achieve shape equilibrium. Wrapping in gold foils minimized evaporation losses at 850 °C, and was critical for the islands to achieve shape equilibrium. The brief exposure to air, between the removal of island samples for wrapping in gold foil and their reinsertion in the UHV system, led to slight contamination of the surfaces with carbon, as determined by AES. However, because the islands are in contact with graphite substrates, subsequent heating to 850 °C produces an equilibrium carbon coverage, which is no different from that obtained in the absence of the brief air exposure. No other contamination of the surface due to air exposure was identified. After shape equilibration, the samples were rapidly cooled to room temperature and transferred to a scanning electron microscope (SEM) for determination of the contact angle. In view of the long equilibration times required at 850 °C, no change in the shape of the particles is expected at room temperature after removal from the UHV environment.

The shape of the equilibrated islands was found to be generally spherical with small flat facets occurring in the vicinity of the {100} and {111} orientations. Contact angles were determined from scanning electron micrographs taken on samples tilted by 70°–80° to the microscope axis. Because a sphere projects as a circle when viewed from any direction, the radius of curvature, R , of the spherical portion of the island surfaces can readily be obtained from any tilt angle. The circular portion of the projection of the island edge on the micrograph was digitized, and fitted to a circle, in order to extract the required radius. In addition, it was possible to measure the diameter, L , of the circular contact between the island and the substrate from the photomicrographs. From these measurements, it was possible to calculate the contact angle, θ , from

$$\theta = \cos^{-1}(L/2R) + 90^\circ \quad \text{for } \theta > 90^\circ \quad (3)$$

In the present study, contact angles were measured for ten different islands and the average value used in later evaluations. The scatter in contact angle values was found to be quite small, the standard deviation being of the order of one degree.

3.3. Crater-edge profiling experiments

These studies were performed on equilibrated thin-film alloy samples. Samples were introduced into

a scanning Auger microprobe (SAM). Because the focus of this part of the study was the composition of the Au(Ni)/graphite interface, the brief exposure to air between the UHV system and the SAM is not considered to be significant. This is because the interface to be studied is protected during passage through air by the thin film on one side and the substrate on the other. The experimental procedure involved argon ion-beam sputtering of the film until a crater was formed to reveal the underlying graphite substrate. Because the ion beam is about 1 mm in diameter and the film is only about 1 μm thick, the crater formed is very shallow. From the geometry of the crater, it is possible to deduce that the angle between the film at the crater edge and the graphite substrate is of the order of milliradians. Consequently, an intercept of the interface along the crater surface is about 10^3 times larger than its thickness. This makes it possible for an Auger line scan taken across the crater edge to detect any segregation at the alloy/graphite interface, if it is present. Fig. 2 gives a schematic illustration of the crater-edge profiling experiment. The Auger data were quantified using the formalism due to Seah [12] for the determination of fractional monolayer coverage at the interface.

3.4. Surface segregation experiments

In the case of Au(Ni) on graphite, both carbon and nickel were found to segregate to the free surface. The surface segregation of these components will affect the surface energy of the alloy. Therefore, in the computation of interfacial energy using the Young–Dupré equation, it was important to use the surface energy as modified by the presence of this segregation.

In order to determine the surface composition, thin films of Au(Ni)/graphite were introduced into the SAM and cleaned by argon-ion sputtering at room temperature. They were then equilibrated at different temperatures in the range 300–540 °C. The Lea and Seah formalism [13] was used to determine the equilibration times at each temperature. Surface concentrations of nickel and carbon were determined using Auger electron spectroscopy. The free energies of segregation of both carbon and nickel to the gold surface were determined using McLean's isotherm [14]

$$\frac{X_i^s}{1 - X_i^s} = \frac{X_i^b}{1 - X_i^b} \exp\left(-\frac{\Delta G_i^{\text{seg}}}{RT}\right) \quad (4)$$

where X_i^s , X_i^b and ΔG_i^{seg} are the surface atom fraction, the bulk atom fraction and the free energy of surface segregation of the i th component ($i = \text{Ni}, \text{C}$), respectively. The changing solubilities of nickel and carbon at different temperatures were taken into account in this analysis. Using the heat of segregation and McLean's isotherm, the concentrations of carbon and nickel at the gold surface at 850 °C were determined. From this, the modified surface energy of gold was determined by applying the Gibb's adsorption isotherm [10] to the gold surface, and this value was subsequently used in the Young–Dupré equation for the determination of the interfacial energy.

4. Results and discussion

From comparisons of wetting studies performed on the gold/graphite and Au(Ni)/graphite interfaces, it was found that addition of 15 at % Ni to gold causes a lowering of the contact angle by about 8°. This is illustrated in Table I, which gives the mean values of the contact angles with their respective standard deviations.

Figs 3 and 4 show photomicrographs of gold islands (with 0 and 15 at % Ni, respectively) equilibrated on graphite. The fact that no nickel adsorbs on the free graphite surface is illustrated in Fig. 5, which is an Auger spectrum taken from the graphite surface following dewetting of an Au(Ni) film. This spectrum does not show any detectable nickel peak. On the other hand, Fig. 6, which is an Auger spectrum taken from the surface of a Au(Ni) island at 400 °C, demonstrates that carbon and nickel segregate to the gold surface at that temperature. Figs. 7 and 8 show the results of carbon and nickel segregation to the gold

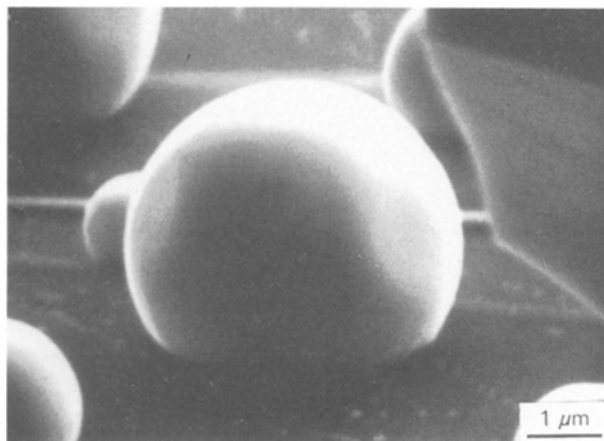


Figure 4 Scanning electron micrograph of Au-15 at % Ni on graphite.

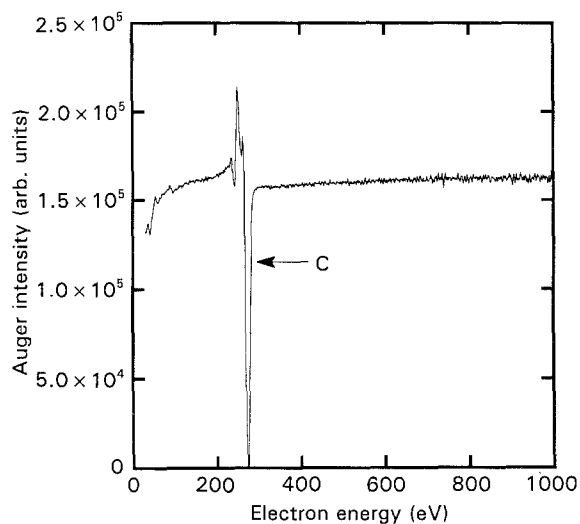


Figure 5 Auger spectrum acquired from free graphite substrate following dewetting of Au-15 at % Ni film and subsequent equilibration.

TABLE I Contact angle of Au-15 at % Ni/graphite compared to gold/graphite

Nickel (at %)	Mean contact angle (deg)	Standard deviation (deg)
0	131	0.77
15	123.2	1.42

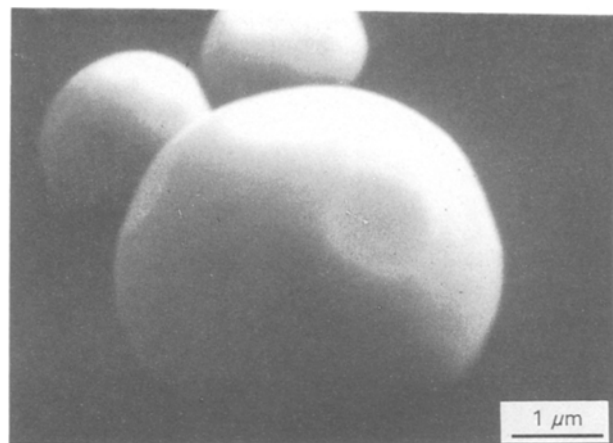


Figure 3 Scanning electron micrograph of pure gold on graphite.

surface at various temperatures up to 540 °C. From the surface segregation experiments, the heats of segregation of carbon and nickel to the gold surface were determined to be -92 and -37 kJ mol^{-1} , respectively. Similarly the entropies of segregation of carbon and nickel to the gold surface were determined to be -40 and $-28 \text{ J mol}^{-1} \text{ K}^{-1}$, respectively. From the free energy of surface segregation determined for carbon and nickel, the surface atom fractions of carbon and nickel at the gold surface at 850 °C were calculated to be 0.043 and 0.25, respectively. The presence of nickel and carbon on the gold surface caused a lowering of the gold surface energy by $\sim 25 \text{ mJ m}^{-2}$, as determined by the application of Gibb's adsorption isotherm to the gold surface. It is of interest to note that the surface segregation of nickel and carbon decreases the surface energy, and leads to an increase in contact angle by 0.9° as calculated using the Young–Dupré equation. Thus the effective change of contact angle due to interfacial segregation of nickel above is 8.7°. Table II summarizes how the surface energy of the Au-15 at % Ni alloy is modified in

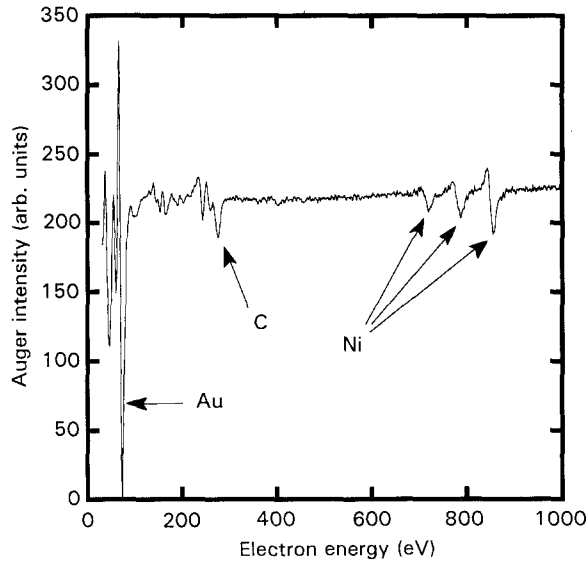


Figure 6 Auger spectrum acquired from the surface of Au-15 at % Ni equilibrated on graphite.

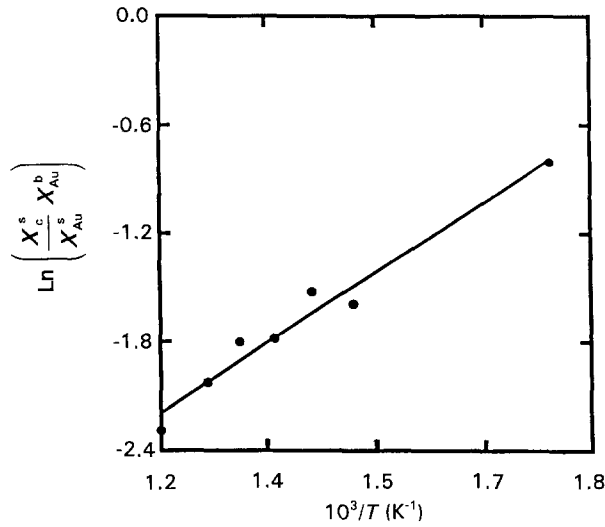


Figure 7 Segregation behaviour of carbon to the free gold surface in the Au-15 at % Ni alloy as a function of temperature.

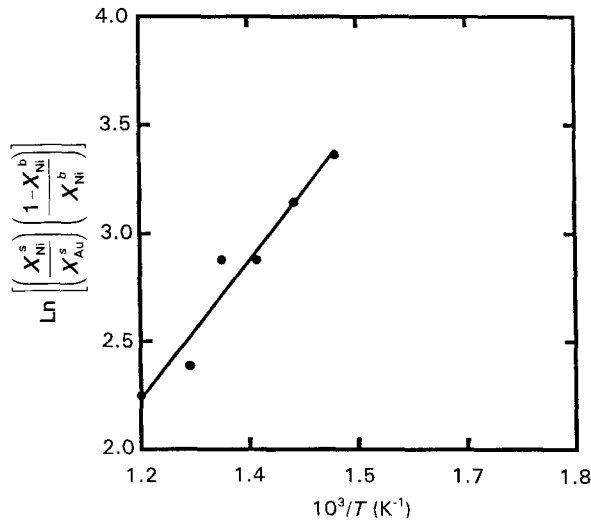


Figure 8 Segregation behaviour of nickel to the free gold surface in the Au-15 at % Ni alloy as a function of temperature.

TABLE II Surface energies of pure gold, Au(C) and Au(C, Ni)

Forms of gold	Surface energy (mJ m ⁻²)
Pure gold [17]	1410
Gold saturated with carbon	1402
Gold-15 at % Ni saturated with carbon	1385

TABLE III Interfacial energy, interfacial excess and number of interfacial monolayers of nickel as obtained from wetting data

Ni (at %)	Interfacial energy (mJ m ⁻²)	Interfacial excess, Γ 10 ⁻⁵ (mol m ⁻²)	Monolayers of nickel at interface
0	1025	0	0
15	913	0.724	0.45

relation to pure gold, as a result of the surface segregation of nickel and carbon.

Table III gives the gold/graphite interfacial energies calculated using the Young-Dupré equation, the contact angle data and the modified surface energy of gold. The Gibb's adsorption isotherm as applied to a two-phase three-component system was used to determine the interfacial excess from the interfacial energy data. The Gibb's adsorption isotherm at the interface takes the following form [15]

$$\frac{d\gamma_{\text{int}}}{d\mu_{\text{Ni}}} = -\Gamma_{\text{Ni}} - \Gamma_{\text{Au}} \left(\frac{X_{\text{Ni}}^{\text{Au}} X_{\text{C}}^{\text{C}} - X_{\text{C}}^{\text{Au}} X_{\text{Au}}^{\text{C}}}{X_{\text{C}}^{\text{C}} X_{\text{Au}}^{\text{Au}} - X_{\text{C}}^{\text{Au}} X_{\text{Au}}^{\text{C}}} \right) - \Gamma_{\text{C}} \left(\frac{X_{\text{Ni}}^{\text{C}} X_{\text{Au}}^{\text{Au}} - X_{\text{Ni}}^{\text{Au}} X_{\text{Au}}^{\text{C}}}{X_{\text{C}}^{\text{C}} X_{\text{Au}}^{\text{Au}} - X_{\text{C}}^{\text{Au}} X_{\text{Au}}^{\text{C}}} \right) \quad (5)$$

where Γ_i is the interfacial excess of the i th component, X_i^j is the atom fraction of the i th component in the j th phase, μ_{Ni} is the chemical potential of nickel, and γ_{int} is the Au(Ni)/graphite interfacial energy.

The above equation can be simplified because of the negligible solubility of gold and nickel in the graphite phase. In addition, it is possible to take $\Gamma_{\text{Ni}} = -\Gamma_{\text{Au}}$, because of the substitutional nature of the Ni-Au alloy. Thus the above equation simplifies to

$$\frac{d\gamma_{\text{int}}}{d\mu_{\text{Ni}}} = -1.176 \Gamma_{\text{Ni}} \quad (6)$$

and can be rewritten as

$$\Delta\gamma_{\text{int}} = -RT 1.176 \int \Gamma_{\text{Ni}}^{\text{int}} d \ln a_{\text{Ni}} \quad (7)$$

where a_{Ni} is the activity of nickel in the gold phase. This expression relates the change in interfacial energy (already determined using the Young-Dupré equation) to the surface excess of nickel at the interface given by $\Gamma_{\text{Ni}}^{\text{int}}$. Discrete values of the dependence of a_{Ni} on composition were obtained from Hultgren *et al.* [16], and fitted to a polynomial which was inserted into the above integral. The resulting expression required numerical integration to yield a value of $\Gamma_{\text{Ni}}^{\text{int}}$. In these computations, it was assumed that nickel atoms

are present at gold lattice sites at the interface. Thus, the interfacial concentration of nickel is reported in equivalent gold monolayers. Table III gives the interfacial excess, Γ_{Ni}^{int} , and the number of monolayers of nickel adsorbed at the interface at the Au-15 at % Ni alloy/graphite interface.

The above procedure provides an indirect method for determining the concentration of nickel at the Au(Ni)/graphite interface. The presence of nickel at this interface was also confirmed by direct measurement in the crater-edge profiling experiments. A clear nickel peak was found at the exposed interface, as shown in Fig. 9a and b, which illustrate a typical crater-edge profiling result. Table IV shows the number of monolayers of nickel at the Au/graphite interface for the Au-15 at % Ni sample as determined from the crater-edge profiling experiment.

It is worth noting that during thin-film deposition, nickel was not deposited on the graphite directly. However, at equilibrium, nickel finds its way to the interface. The crater edge profiling results yield a larger value of interfacial nickel segregation (0.74 monolayers) than that inferred from the wetting studies (0.45

TABLE IV Number of interfacial monolayers of nickel as determined from crater-edge profiling experiments

Nickel (at %)	Monolayers of nickel at interface
0	0
15	0.74

monolayers). This discrepancy is most likely due to differential sputter yields, and sputter-induced mixing caused by the ion beam. In general, obtaining quantitative composition profiles from sputter depth profiling requires complex data deconvolution. Therefore, the discrepancy found here is not surprising. While this experiment clearly establishes the presence of nickel at the interface, it also establishes the absence of impurities such as oxygen, sulphur, etc., at the gold/graphite interface, within the detection sensitivity of Auger spectroscopy. Thus it is appropriate to relate all of the change in interfacial energy to nickel segregation.

The results clearly demonstrate that the contact angle of gold supported on a graphite substrate is reduced by nickel additions to gold. It has been mentioned earlier that nickel has a positive free energy of carbide formation at temperatures of interest, which implies that there is no thermodynamically stable carbide possible. This is confirmed by the absence of nickel on the free graphite substrate following dewetting, as seen from the Auger spectrum in Fig. 5. It is found that both nickel and carbon segregate to the free gold surface and that nickel segregates to the gold/graphite interface. While surface segregation of nickel and carbon have an effect on contact angle (an increase by 0.9°), the major contribution to the contact angle change is due to segregation of nickel at the gold/graphite interface.

While the lowering of interfacial energy due to interfacial nickel segregation is significant, the observed contact angle change is not very large. The low sensitivity of the contact angle change to significant changes in interfacial energy in this case is a consequence of the relatively large surface energy of pure gold.

5. Conclusion

The addition of 15 at % nickel to gold supported on graphite has been found to cause a lowering of contact angle by 7.8° . The corresponding change in interfacial energy was found to be 112 mJ m^{-2} . Nickel segregates to both the free gold surface and the gold/graphite interface. In addition, carbon is found to segregate to the free gold surface. The presence of carbon and nickel at the free gold surface leads to a lowering of surface energy by $\sim 25 \text{ mJ m}^{-2}$, and results in an increase in contact angle by $\sim 0.9^\circ$. Thus the effective lowering of contact angle due to interfacial adsorption of nickel is 8.7° . The interfacial nickel concentration associated with a decrease in contact angle is determined to be 0.45 monolayers. The presence of nickel at the interface is confirmed qualitatively by crater edge profiling studies.

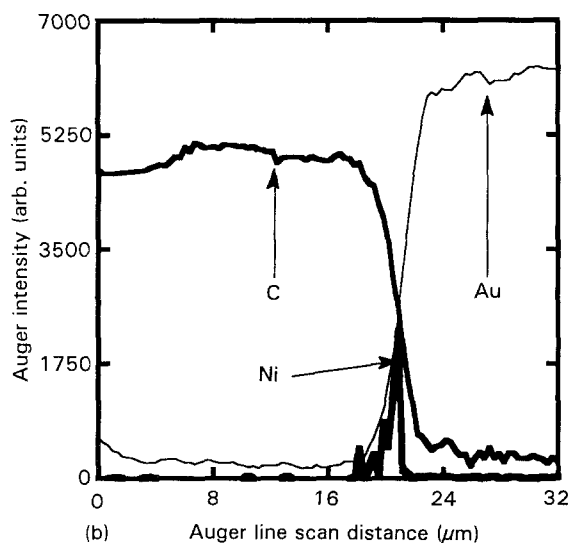
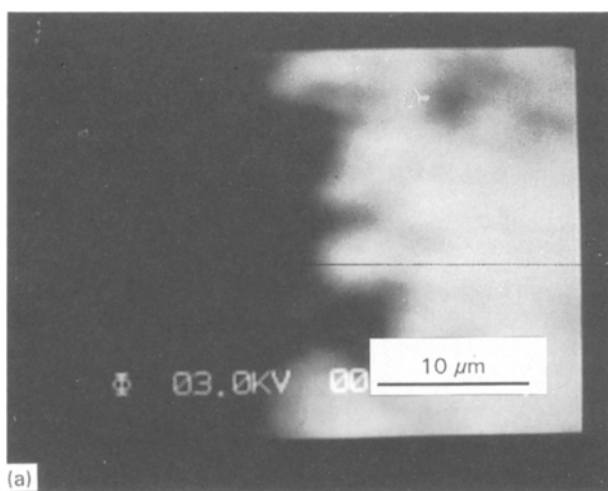


Figure 9 (a) Scanning electron micrograph of the line-scanned region during crater-edge profile studies. (b) Line scan results corresponding to (a) showing concentration profiles of gold, carbon and nickel.

References

1. JU. V. NAIDICH, *Prog. Surf. Membrane Sci.* **14** (1981) 353.
2. J. E. RITTER Jr and M. S. BURTON, *Trans. Met. Soc. AIME* **239** (1967) 21.
3. P. KRITSALIS, L. COUDURIER and N. EUSTATHOPOULOUS, *J. Mater. Sci.* **26** (1991) 3400.
4. D. A. MORTIMER and M. NICHOLAS, *ibid.* **5** (1970) 149.
5. D. EVENS, M. NICHOLAS and P. M. SCOTT, *Ind. Diamond Rev.* **307** (1977) 6.
6. U. GANGOPADHYAY and P. WYNBLATT, *Metall. Mater. Trans.* **25A** (1994) 607.
7. G. TAMMAN and W. OELSEN, *Z. Anorg. Chem.* **186** (1930) 266.
8. M. SINGLETON and P. NASH, *Bull. Alloy Phase Diag.* **10** (1989) 121.
9. F. A. NICHOLS and W. W. MULLINS, *Trans. AIME.* **233** (1965) 1840.
10. J. W. GIBBS "The Scientific Papers of J. Williard Gibbs" (Dover, New York, 1961).
11. W. JOST, "Diffusion in Solids, Liquids and Gases" (Academic Press, New York, 1960).
12. M. P. SEAH, in "Practical Surface Analysis by Auger and X-Ray Photoelectron Spectroscopy". edited by D. Briggs and M. P. Seah (Wiley, New York, 1983) p. 181.
13. C. LEA and M. P. SEAH, *Philos. Mag.* **35** (1977) 213.
14. D. McLEAN, "Grain Boundaries in Metals" (Oxford University Press, Oxford 1957).
15. R. DEFAY, I. PRIGOGINE, A. BELLMAN and D. H. EVERETT, "Surface Tension and Adsorption" (Wiley, New York, 1966).
16. R. HULTGREN, P. D. DESAI, D. T. HAWKINS, M. GLEISER and K. K. KELLEY, "Selected Values of the Thermodynamic Properties of Binary Alloys", ASM 295 (ASM, Metals Park 1973).
17. V. K. KUMIKOV and KH. B. KHOKONOV, *J. Appl. Phys.* **54** (1983) 1346.

*Received 16 December 1993
and accepted 9 June 1994*